Human Plague Risk: Spatial-temporal Models

J.E. Pinzon
Science Systems and Applications, Inc (SSAI)/NASA GSFC, Code 614.4, Greenbelt, MD, USA

Plague is a highly virulent flea-borne zoonotic disease maintained in nature as an infection of rodents, typically ground squirrels, prairie dogs, chipmunks or woodrats. Its etiological agent, *Yersinia pestis*, is considered one of the most pathogenic bacteria for humans. Plague is usually transmitted to humans by the bites of infected rodent fleas, less often by handling of infected animals and rarely by direct airborne spread (Dennis and Meier 1997, Gage 1998, Parmenter et al. 1999, Gage and Kosoy 2005). It remains endemic in many parts of the Americas, Asia and Africa and it is characterized by quiescent and epizootic periods that usually precede the majority of human cases with increased depopulation of affected rodents, probably forcing the dispersal of infected fleas in search of new hosts (Perry and Fetherston 1997, Levy and Gage 1999, Stapp et al. 2004). Phenotypically, there are three *Y. pestis* biotypes that caused three infamous pandemics: Antiqua – that caused the Justinian plague, the first pandemic in the 6th century AD; Mediavalis – the Black Death or Great Pestilence, the second pandemic in the 14th century; and Orientalis – that caused the third pandemic in the 19th century (Torrea et al. 2006, Clam and Galwankar 2005). The Orientalis pathogen was introduced to the United States around 1900 through marine shipping from plague-endemic regions of Asia by infected rats and fleas and then spread through North- and South-America. Today, Orientalis is the dominant strain with almost worldwide distribution and has likely been the only source of all endemic cases in the continent. The two other biotypes have a geographically restricted distribution: Mediavalis in Asia and Antiqua in some parts of Africa and in Central Asia. In any case, the World Health Organization listed plague as an international quarantine reemerging disease with the status of category one biological weapon since it has been reappearing in areas plague-free (Daszak et al. 2000, WHO 2004, Clem and Galwankar 2005, Wolf et al. 2007).

In United States, there are still occasional human cases of plague diagnosed in the western states with fatality rates remaining high (CDC 2003). Most of the human cases occur in a peridomestic environment and are reported from the four-corners region, 83% of 416 total cases since 1950 (CDC 2006, Eisen et al 2007A), which includes the states of Arizona, Colorado, New Mexico, and Utah. Mortality rates for untreated plague infections range from 40 to 70% for bubonic to almost always fatal for pneumonic or septicemic infection (Levy and Gage 1999). Little is known about the dynamics of plague in its natural reservoirs, particularly about the survival strategies of *Y. pestis* (Perry and Fetherston 1997, Gage and Kosoy 2005). Yet effective rodent control and prompt diagnosis followed by appropriate antibiotic treatment have greatly reduced the morbidity and mortality from the disease (Levy and Gage 1999, CDC 2003, 2006; Gage and Kosoy 2005). Thus, informed pre-emptive decisions about plague management and prevention preceding outbreaks would certainly be more sustainable and cost-beneficial than the usual

"fire-fighting" approach – only when an epidemic occurs, implement emergency response plans, but by then it is usually too late to have any impact on transmission (Stenseth et al. 2008). The natural cycles of plague are conditioned by features of the ecology, environment, host, agent, factors which vary temporally and spatially. Recent studies have identified local climatic factors and landscape features associated with increased plague activity. In Arizona and New Mexico, epizootic activity intensifies when cool summer temperatures follow wetter winter-spring seasons (Parmenter et al. 1999, Enscore et al. 2002). When favorable climatic conditions occur, assuming a trophic cascade of (climatological, ecological and demographic) events (Yates 2002), they can lead to increases in the population of the rodent hosts and flea vectors and as a consequence they can lead to a higher risk for human exposure. Several limitations hindered these temporal models to be used as predictive models. One of the most limiting factors is their sensitivity to spatial heterogeneity that makes unlikely the ability of a good generalization.

Earth observation by satellite remote sensing over nearly thirty years has enabled systematic analysis and mapping of the close coupling between vectors of disease and the driver indicators of climate variability, e.g. El Niño/Southern Oscillation (ENSO), rainfall, temperature and vegetation, on a global scale at high-temporal and moderate spatial resolutions (Linthicum et al. 1999, Beck et al. 2000, Pinzon et al. 2005a, Anyamba et al. 2009). More recently these tools has been used to expand our knowledge of the coupling between plague and climate. Logistic regression models were used within the four-corners region to identify local landscape features associated with human plague cases and to create a predictive geographical model of high-risk habitats for human exposure to *Y. pestis* (Eisen et al. 2007A, Eisen et al. 2007B). Although these spatial models were not intended to be predictive in the temporal domain, they provided a fine-scale modeling of adjacent spatial interactions between landscape elements and the ability to predict where infections are likely to occur, albeit in limited areas. These models relate the risk of exposure to *Y. pestis* to suitable environmental indicators using occurrence-only data from the contact rates between humans and the infectious agent. Even though the epidemiological data is of high quality, we cannot equate absence with unsuitability. Nonetheless, these studies provide some useful insights into those aspects of incorporating explicit ecological features to improve our understanding and prediction of disease risk that cannot be treated in previous models. Prior to the classification, the landscape and climatic features associated with human risk to exposure to *Y. pestis* included elevation and 4 quarterly means of NDVI seasonal profiles for each 8km grid cell. The stepwise optimal hierarchical clustering (SOHC) approach can be applied to identify training samples that contribute the most in the cluster classification and optimize criterion functions (Duda et al 2000). The climatic, landscape and ecological properties of these samples can be used to identify and generalize temporal characteristics of plague outbreaks in the region (Figure 1). These features were selected for being the most valuable and robust from a larger set of candidate features, e.g. monthly variance of NDVI seasonal profiles, land-cover habitat type, and monthly mean of temperature and rainfall profiles (Pinzon et al. 2005a). Moreover, on a seasonal scale, natural vegetation (given by NDVI) is well correlated with climate variables including rainfall, evapo-transpiration and surface temperature in a wide range of environmental conditions. When these features are viewed from different timescales using the method of empirical mode decomposition (Huang et al. 1998, Pinzon et al 2005b, Huang et al. 2009)[1], we can revisit the links between climate (El Niño/Southern Oscillation

[1] The most commonly used ENSO indices are the Southern Oscillation Index (SOI) computed from the Darwin and Tahiti pressure difference and indices based on sea surface temperature on several regions of the equatorial Pacific Ocean: R12 (0-10S,80-90W), R3 (5S-5N,150W-90W), R4 (5S-5N,160E-150W), and R3.4 (5S-5N,170W-120W). We can monitor ENSO through the Multivariate ENSO Index (MEI) that is a multivariate measure of the ENSO signal as expressed in the first principal component of six observed variables from the tropical Pacific Comprehensive Ocean-Atmosphere data set (COADS): sea level pressure, surface zonal and meridional wind components, sea surface temperature, surface air temperature and cloudiness (Wolter and Timlin 1998). MEI is

(ENSO)) and plague epizootics in the region To start, we relate the last 3 IMFs components of the MEI signal (IMF_{4-6}) lagged 12 months with the time series of number of cases given by quarters (Figure 2). The overall result is that incidence of plague is explained by positive ENSO years as shown implicitly in Figure 2. The first two principal components of the correspondence analysis explain 98% of the variance of the category matrix (Pinzon et al. 2010). Two salient features are apparent: a distinct contribution to the total number of cases and when this contribution peaks in each cluster. Each cluster contributes different amounts to the total number of cases making possible a new tool to rank plague risk: C1 (8%), C2 (26%), C3 (13%), C4 (20%), and C5 (33%). Our ability to target limited prevention resources would also improve if we mask the risk maps with a density population map of the region (Figure 7). The plague endemic area is thus concentrated on peridomestic regions that constitute about 85% of the cases. Moreover, using the climatic and ecological features to extend globally the SOHC model, we can identify and validate common characteristics of endemic plague regions (Figure 4). 79% of the cases (C5+C2+C4) occur in regions where NDVI is lower than 0.4 with and average elevation less than 2000 m. Thus, the early recognition and improving management of plague provided by these models have underscored the importance of an even better understanding of the (spatio-temporal) conditions that give rise to the emergence of plague in both human and animal populations and of developing critical tools to make plague surveillance more comprehensive and timely in order to prevent or minimize the potential for human outbreaks. This kind of system could operate in near real-time to monitor plague risk on a monthly basis and could offer the opportunity to identify eco-climatic conditions associated with potential vector-borne disease outbreaks over large areas. Still, many aspects of this subject are still ripe for further investigation and improvement.

REFERENCES

Anyamba, A., Chretien, J.P., Small, J., Tucker, C.J., Formenty, P.B., Richardson, J.H., Britch, S.C., Schnabel, D.C., Erickson, R.L., &Linthicum, K.J., 2009. Prediction of a Rift valley fever outbreak. *PNAS* 105:955-959.

Beck, L.R., Lobitz, B.M., & Wood, B.L., 2000. Remote sensing and human health: New sensors and new opportunities. *Emerg Infect Dis* 6: 217-227.

CDC, 2003. Imported plague – New York City, 2002. *MMWR 2003* Aug 8; 52: 725-728.

CDC, 2006. Human plague—Four states, 2006. *MMWR 2006* Aug 25; 55: 1-3.

Clem, A., & Galwankar, S., 2005. Plague a decade since the 1994 outbreaks in India. *JAPI 53*: 457-464.

Craven, R.B., Maupin, G.O., Beard, M.L., Quan, T.J., & Barnes, A.M., 1993. Reported cases of human plague infections in the United States, 1970–1991. *J Med Entomol 30:* 758–761.

Daszak, P., Cunningham, A.A, & Hyatt, A.D., 2000. Emerging Infectious Diseases of Wildlife—Threats to Biodiversity and Human Health. *Science 287:* 443-449.

Dennis, D., & Meier, F., 1997. Plague. In: Horsburgh CR, Nelson AM, eds. Pathology of emerging infections. Washington, DC: ASM Press, 21-47.

Eisen, R.J., Enscore, R.E., Biggerstaff, B.J., Reynolds, P.J., Ettestad, P., Brown, T., Pape, J., Tanda, D., Levy, C.E., Engelthaler, D.M., Cheek, J., Bueno, R., Targhetta, J., Montenieri, J.A., & Gage, K.L., 2007A. Human plague in the southwestern United States, 1957-2004: spatial models of elevated risk of human exposure to Yersinia pestis. *J Med Entomol 44* (3):530-537.

Eisen, R.J., Reynolds, .P.J, Ettestad, P., Brown, T., Enscore, R.E., Biggerstaff, B.J., Cheek, J., Bueno, R., Targhetta, J, Montenieri, J.A., & Gage, K.L., 2007B. Residence-Linked Human Plague in New Mexico: .A Habitat-Suitability Model. *Am J Trop Med Hyg.. 77*:121-125.

Enscore, R.E., Biggerstaff, B.J., Brown, T.L., Fulgham, R.F., Reynolds, P.J., Engelthaler, D.M., Levy, C.E., Parmenter, R.R., Montenieri, J.A., Cheek, J.E., Grinnell, R.K., Ettestad, P.J., & Gage, K.L., 2002.

---

re-computed every month to monitor the strength of ENSO conditions since 1950. Correlations between the MEI and other most common indices range from 0.8 and 0.9 (Wolter and Timlin 1998).

Modeling relationships between climate and the frequency of human plague cases in the southwestern United States, 1960-1997. *Am. J. Trop. Med. Hyg. 66*:186-196.

Gage, K.L., 1998. Plague. Colier L, Balows A, Sussman M, eds. *Topley and Wilson's Microbiology and Microbial Infections*. Oxford, United Kingdom: Oxford University Press. 885–904.

Gage, K.L., & Kosoy, M.Y., 2005. Natural history of plague: perspectives from more than a century of research. *Annu Rev Entomol 50:* 505–528.

Huang, N.E., Shen, Z., Long, S.R., Wu, M.C., Shih, E.H., Zheng, Q., Tung, C.C., & Liu, H.H., 1998. The empirical mode decomposition method and the Hilbert spectrum for non-stationary time series analysis. *Proc. Roy. Soc. London* 454A: 903–995.

Huang N.E., Wu, Z., Pinzon, J.E., Parkinson, C.L., Long, S.R., Blank, K., Gloersen, P., & Chen, X., 2009. The empirical mode decomposition method and the Hilbert spectrum for non-stationary time series analysis, *Proc. Roy. Soc. London* 454A: 903–995.

Levy, C.E., & Gage, K.L., 1999. Plague in the United States, 1995-1997. *Infect. Med.* 16: 54-64.

Linthicum, K.J., Anyamba, A., Tucker, C.J., Kelley, P.W, Myers, M.F, & Peters C.J, 1999. Climate and satellite indicators to forecast Rift Valley Fever epidemics in Kenya. *Science* 285:397-400.

Parmenter, R.R., Yadav, E.P., Parmenter, C.A., Ettestad, P.J., & Gage, K.L., 1999. Incidence of plague associated with increased winter-spring precipitation in New Mexico. *Am J Trop Med Hyg* 61: 814-821.

Perry, R.D., & Fetherston, J.D., 1997. Yersina pestis—etiologic agent of plague. Clin Microbiol Rev 1997 Jan;10(1):35-66.

Pinzón, J.E., Wilson, J.M., &Tucker, C.J., 2005a. Climate-based health monitoring for eco-climatic conditions associated with infectious diseases. *Bull. de la Société de Pathologie Exotique*, T.98 (3): 239-243.

Pinzon, J.E., Brown, M.E., & Tucker, C.J., 2005b. Empirical Mode Decomposition Correction of Orbital Drift Artifacts in Satellite Data Stream, Chapter 8, Part II. Applications, in Hilbert-Huang Transform and Applications, Ed. N. E. Huang and S. S. Shen, World Scientific, Singapore, 167-186.

Pinzón, J.E., Eisen, R.J., Enscore, R.E., Reynolds, P.J., Ettestad, P., Brown, T., Pape, J., Tanda, D., Levy, C.E., Engelthaler, D.M., Cheek, J., Bueno, R., Gage, K.L., & Tucker, C.J., 2010a. A Spatial-temporal Model of Human Plague Risk in the Southwestern United States. *In preparation.*

Stapp, P., Antolin, M.F., & Ball, M., 2004. Patterns of extinctionin prairie dog metapopulations: plague outbreaks follow El Niño events. *Front. Ecol.* 2: 235-240.

Stenseth, N.C., Atshabar, B.B., Begon, M., Belmain, S.R., Bertherat, E., Carniel, E., Gage, K.L., Leirs, H., & Rahalison, L., 2008. Plague: Past, Present, and Future. *PLoS* 5: 9-13.

Torrea, G., Chenal-Francisque, V., Leclercq, A., & Carniel, E., 2006. Efficient Tracing of Global Isolates of *Yersinia pestis* by Restriction Fragment Length Polymorphism Analysis Using Three Insertion Sequences as Probes. *J. Clinical Microbiology* 44(6):2084-2092.

Wolf, N.D., Donovan, C.P., & Diamond, J., 2007. Origin of major human infectious diseases. *Nature, 447*:279-283.

Wolter, K., Timlin, M.S., 1998. Measuring the strength of ENSO events: How does 1997/98 rank? *Weather* 53: 315-324. http://www.cdc.noaa.gov/people/klaus.wolter/MEI/mei.html. Last Access February 2009.

World Health Organization. 2004. Human plague in 2002 and 2003. *Wkly. Epid. Rec. 79*:301–306.

Duda, R.O., Hart, P.E., & Stork, D.G., 2000. Pattern classification 2ed., New York: *Wiley-Interscience*.

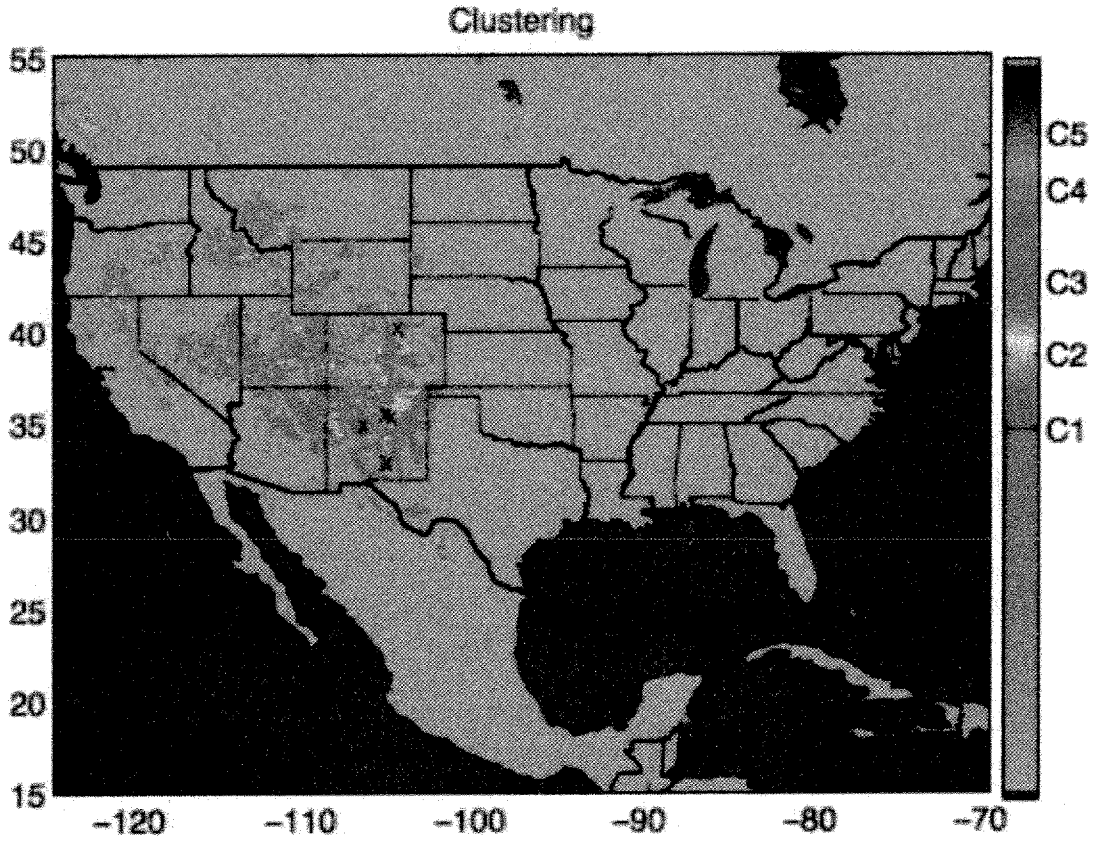

Figure 1. The stepwise optimal hierarchical clustering approach is applied to identify training samples that contribute the most in the cluster classification and optimize criterion functions. The climatic, landscape and ecological properties of these samples are used to identify and generalize temporal characteristics of plague outbreaks in the region. Adapted from Pinzon et al 2010.

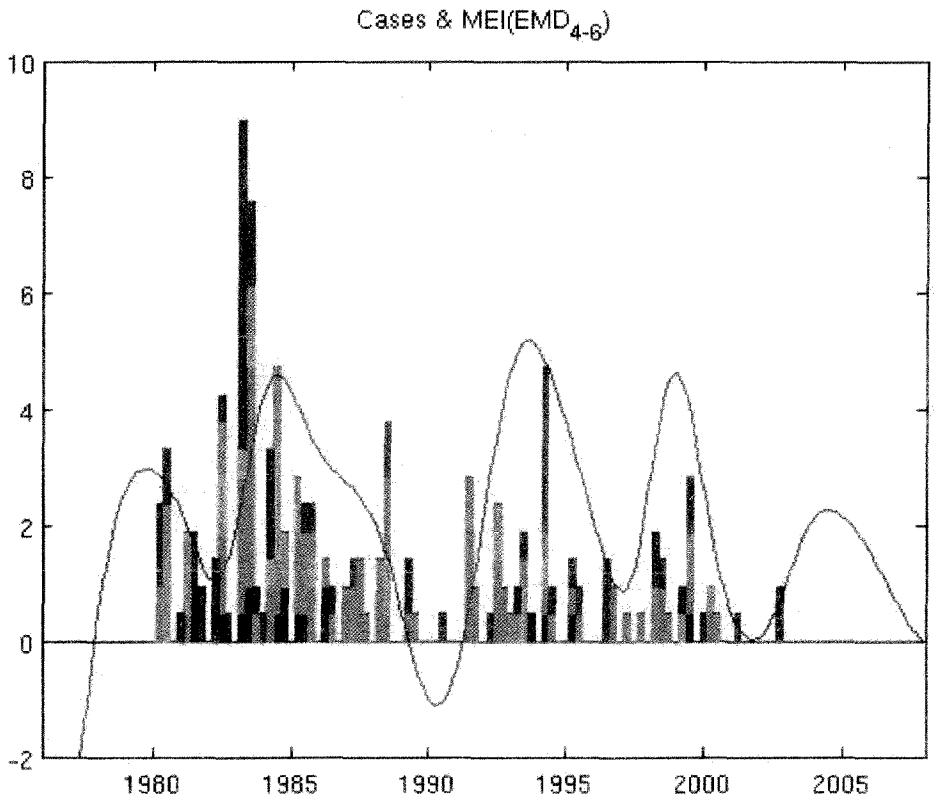

Figure 2. Time series behavior of the NDVI data from the documented outbreak sites of EBOV HFrelate the last 3 IMFs components of the MEI signal (IMF_{4-6},,blue line) lagged 12 months with the time series of number of cases given by quarters and clustered according to SOHC. Adapted from Pinzon et al 2010.

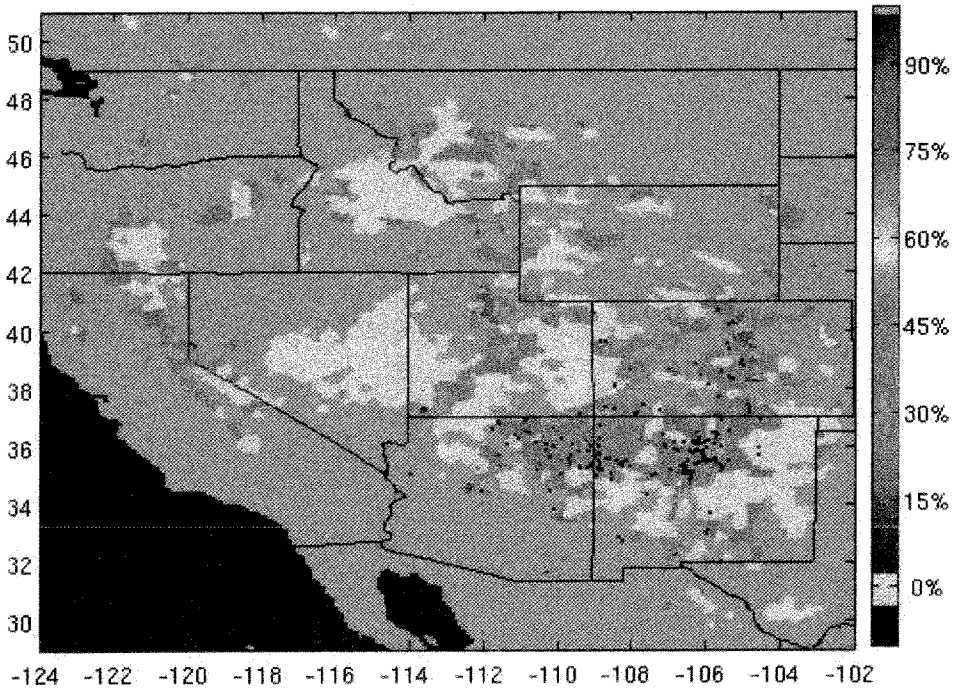

Figure 3. Time series behavior of the NDVI data from the documented outbreak sites of EBOV HF. Note that all outbreaks occur toward the middle of the second dry season. Adapted from Pinzon et al 2004.

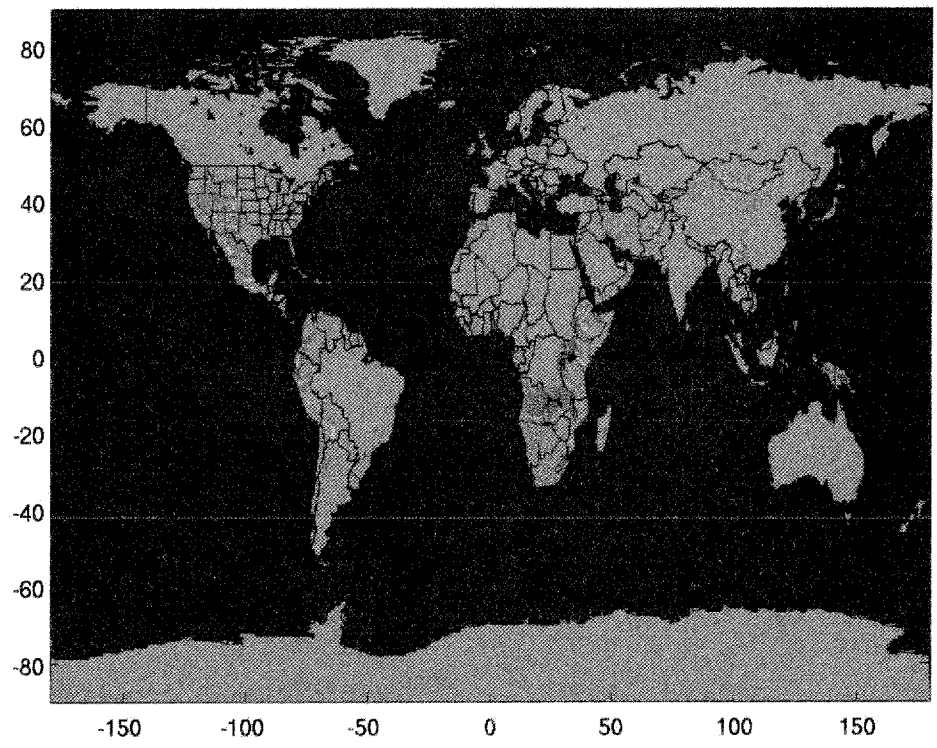

Figure 4. Global extension of the SOHC model based on 5 clusters.